

An Experimental Study of Fluid Forces Applied on a Circular
Cylinder in Air Flow with $1/7$ Power Law Velocity
Distribution through Horizontal and Vertical Duct

Fujio YAMAMOTO* and Hideki MONYA*

(Received Feb. 26, 1988)

The present paper discusses the effects of the velocity gradient of air flow and the clearance between circular cylinder and inner surface of duct wall on the fluid force applied on a circular cylinder immersed in air flow with $1/7$ power law velocity distribution in a horizontal and vertical duct. The pressure distributions on a circular cylinder and duct walls are measured and the pressure lift and drag are analysed, using jointly a pendant method. The conclusions attained are summarized as follows:

- (1) The lift due to the flow velocity gradient is applied in the direction from the side of the higher velocity toward the side of the lower velocity, and increases as the velocity gradient becomes steeper.
- (2) The lift due to the clearance between circular cylinder and duct wall is applied in the opposite direction to the lift due to the velocity gradient, and increases as the clearance becomes smaller.
- (3) The resultant lift due to the velocity gradient and due to the clearance vanishes at a clearance ratio, and turns over the applying direction across it.
- (4) The drag applied on the circular cylinder is almost independent of the velocity gradient.

1. Preface

The present study originated in the demand for the fundamental data to simulate numerically the solid-gas flow in a pipe. Most studies of the numerical simulation employ the data obtained from the experimental studies which were carried out of uniform flows.

* Dept. of Mechanical Engineering

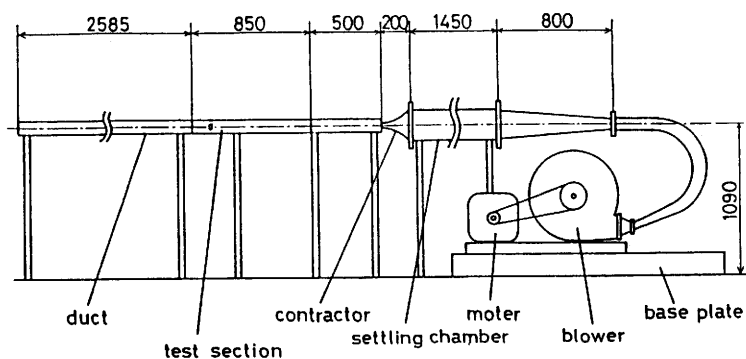


Fig. 1 Horizontal Duct

As everybody knows, the lift force is not applied on a non-rotating axisymmetric particle (sphere or circular cylinder) in a uniform flow. But the lift force is applied on a particle in a pipe flow. Most studies⁽¹⁾⁻⁽⁸⁾ deal with the lift force in laminar flows or turbulent boundary layer flows. There are few studies which discuss the lift force due to the flow velocity gradient and the clearance between the particle and pipe wall in turbulent pipe flows.

The present experiment was carried out, using two ducts, both of which have the same rectangular sections. One is a horizontal type, and the other a vertical type. The air flow in the test ducts presents the $1/7$ power law velocity distribution, which represents the fully developed turbulent flow. The effects of the velocity gradient of air flow and the clearance between circular cylinder and duct wall on the fluid forces applied on a circular cylinder were investigated. The pressure distributions on a circular cylinder and duct walls were measured and the pressure lift and drag are analysed, using jointly a pendant method. The experiment for the measurement of pressure was carried out in the range of the Reynolds number referred to the circular cylinder, $Re = 7000 \sim 14000$, and the experiment by the pendant method in the range $Re = 600 \sim 2000$.

2. Experimental Apparatus and Procedure

2.1 Duct and Flow Field

The horizontal duct is a delivery type, as shown in Fig. 1, and has 40 mm X 200 mm rectangular section with the total length 3935 mm (except the settling chamber). The vertical duct is a suction type, as shown in Fig. 2, and has the same section with the total length 3100 mm as the horizontal duct.

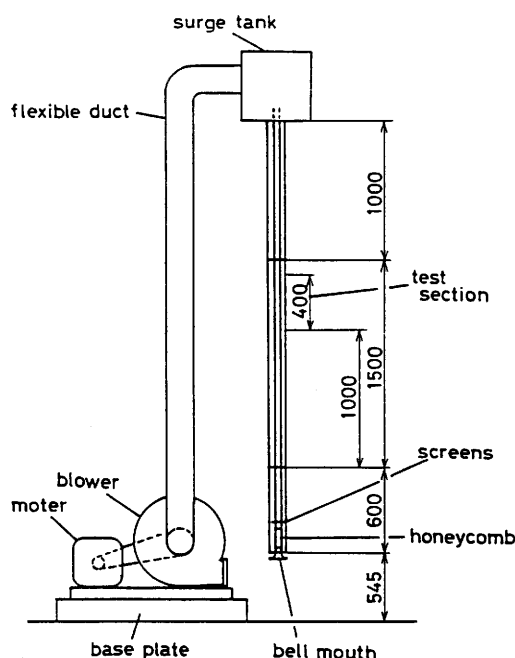


Fig. 2 Vertical Duct

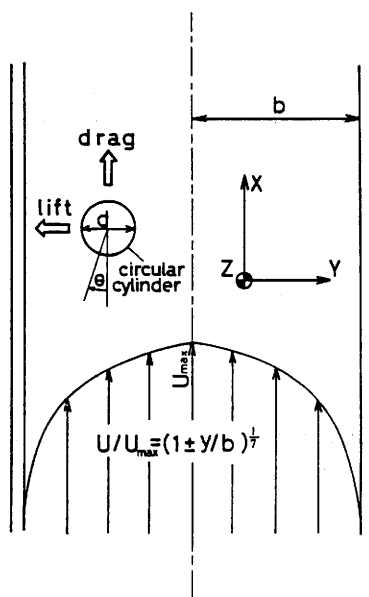
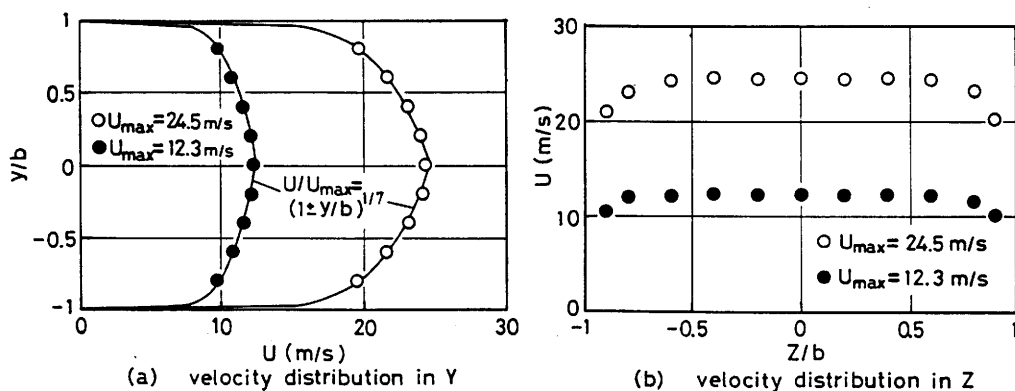


Fig. 3 Coordinate System



(a) velocity distribution in Y

(b) velocity distribution in Z

Fig. 4 Velocity Distributions in a Horizontal Duct

The coordinates of flow field are taken as shown in Fig. 3. The x direction is taken in the direction of the air flow, y in the direction from the side of smaller velocity to the side of greater velocity, and z (spanwise) in the direction perpendicular to both x and y directions. The original point is located on the pipe center line in the section where the test circular cylinder is fixed. The velocity distributions were measured in several sections of the ducts, and the flow field in the test section could be regarded as two dimensional, as shown in Fig. 4.

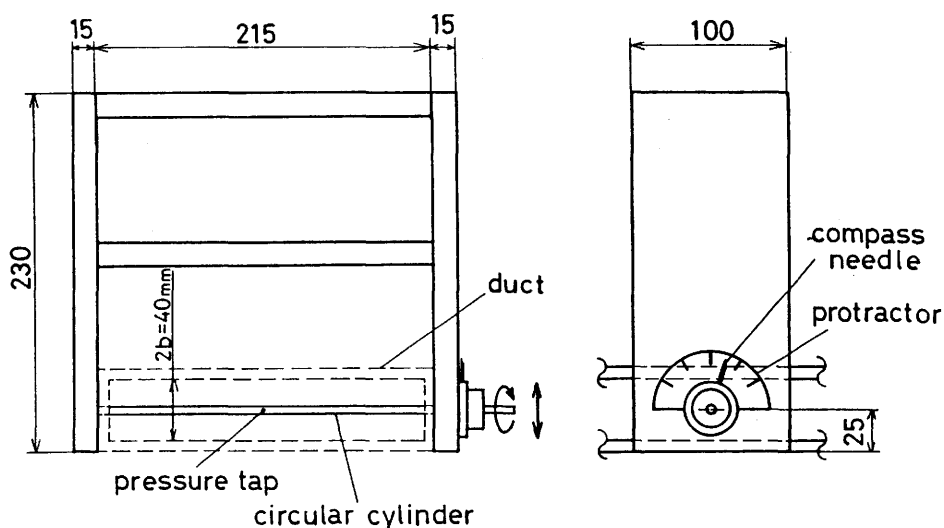


Fig. 5 Device for Measurement of Pressure Distributions on Circular Cylinder

2.2 Measurement of Pressure Distributions on Surfaces of Circular Cylinder and Duct Walls

The pressure distributions on the surface of circular cylinder immersed in the test ducts were measured, using a device as shown in Fig. 5. Two pipes with the diameters $d = 5$ mm and 8 mm are employed as the test circular cylinders. The circular cylinder is located so that its axis is parallel to the z direction, and movable in the y direction so that $y/b = 0, -0.25, -0.5, -0.55, -0.65, -0.7, -0.75, -0.8$. A pressure tap with the diameter 0.8 mm is made at the spanwise center of the circular cylinder, which can be rotated by hand. The pressure is led to a Göttingen type of manometer through the inner hole of the circular cylinder.

The pressure distributions on the upper and lower surfaces of the horizontal duct were measured at 52 points where the static pressure taps are made at intervals of 5 or 10 mm downstream and upstream of the circular cylinder, simultaneously with measurement of the pressure distributions on the surface of the circular cylinder.

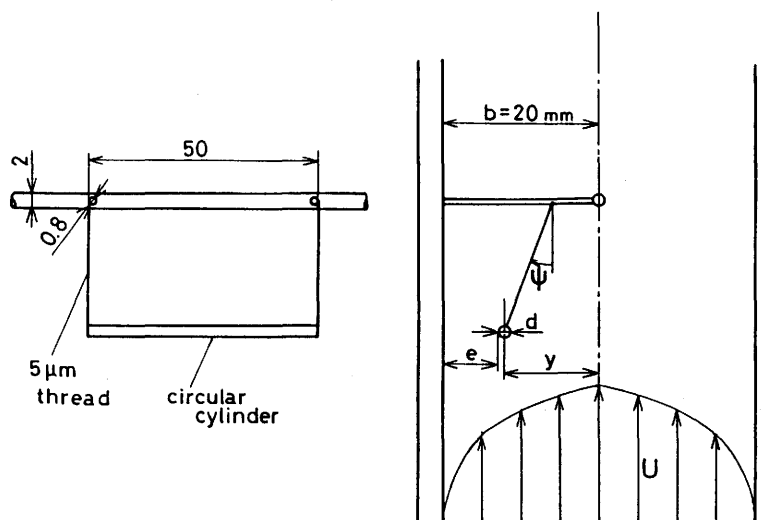


Fig. 6 Pendant System

2.3 Measurement of Lift by Pendant Method

The device for measurement of lift by a pendant method is as shown in Fig. 6. The experiment was carried out in the test section of the vertical duct. The test circular cylinders with the diameter $d = 1 \text{ mm}$, 1.5 mm , and 2 mm and the same length $L = 50 \text{ mm}$ were employed. The aspect ratio L/d for the circular cylinder is greater than 25, and is thought to be enough great to neglect the effects of upwash vortices around the edges of the circular cylinder. The diameter of the silk thread to suspend the circular cylinder is 0.005 mm , and according to a preliminary calculation the force applied on the threads can be regarded as negligible in comparison with the drag and lift applied on the circular cylinder.

The inclination angle ψ of the suspending threads are measured on the photographs taken by a camera with a power winder, using a graphic digitizer.

From the balance of forces, the lift F_L is calculated by the following equation:

$$F_L = (mg - F_D - F_b) \tan \psi \quad (1)$$

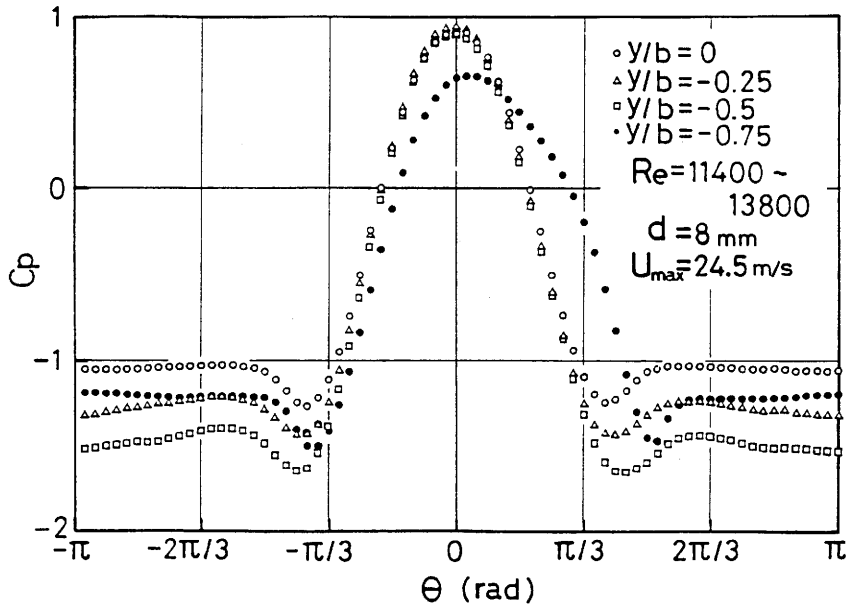


Fig. 7 Pressure Distributions on a Circular Cylinder

where mg is the gravity force, F_b the buoyancy, and F_D the drag. The drag is calculated on the assumptions that the circular cylinder is infinitely long and that the drag coefficient C_D may be given from the $Re - C_D$ chart for the uniform flow. In the calculation of the Reynolds number the velocity of the approaching flow to the leading edge of the circular cylinder is taken for the reference velocity.

3. Results and Discussion

3.1 Pressure Drag and Lift

An example of the pressure distribution on the surface of a circular cylinder with the diameter $d = 8$ mm at the flow velocity $U_{max} = 24.5$ m/s on the duct center line is shown in Fig.7. Here, the pressure coefficient C_p is defined by the following equation:

$$C_p = \frac{P - P_s}{\frac{1}{2} \rho_a U_{cen}^2} \quad (2)$$

θ is the angle around the z axis, as shown in Fig. 3. Naturally, the pressure distribution in the case that the circular cylinder is located on the center of the duct shows the symmetric curve

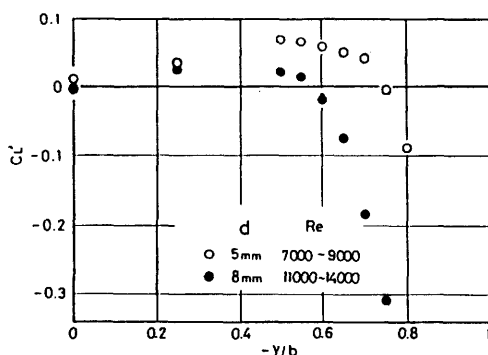


Fig. 8 Lift Coefficient Computed from Pressure Distribution.

about the axis $\theta = 0$. Here, the position that $\theta = 0$ represents the leading edge of the circular cylinder. As the circular cylinder approaches to the lower wall of duct, that is, the value of y decreases from zero to minus, the curves show the pretty asymmetry about the axis $\theta = 0$. For instance, in the case that $y/b = -0.25$ and -0.5 , when one compares the pressures at the same value of $|\theta|$, it is found that the pressures in the negative range of θ from 0 to about $-\pi/3$ are a little higher than those in the positive range of θ from 0 to about $\pi/3$. It is difficult to define the separation points from the pressure distributions, it may be said that the separation points are near the angle $\theta = \pi/3$. The pressure distributions keep symmetry for the range $|\theta| > \pi/3$. Consequently, the asymmetry of pressure distribution causes the lift applied in the direction toward to the wall of duct. On the other hand, in the case that $y/b = -0.75$, that is, when the circular cylinder is very close to the wall, the pressures in the positive range of θ are higher than those in the negative range of it, and the lift is applied in the direction toward to the duct center.

The coefficients of pressure lift and drag (C_D and C_L) are computed by numerical integration of the pressure coefficient [Eq. (2)] as follows:

$$C_D = \frac{1}{2} \oint C_p \cos \theta \, d\theta \quad (3)$$

$$C_L = \frac{1}{2} \oint C_p \sin \theta \, d\theta \quad (4)$$

The dependance of $C_L' = C_L$ and C_D on the y direction is shown in Fig. 8 and Fig. 9, respectively. In the case that the diameter $d=5$

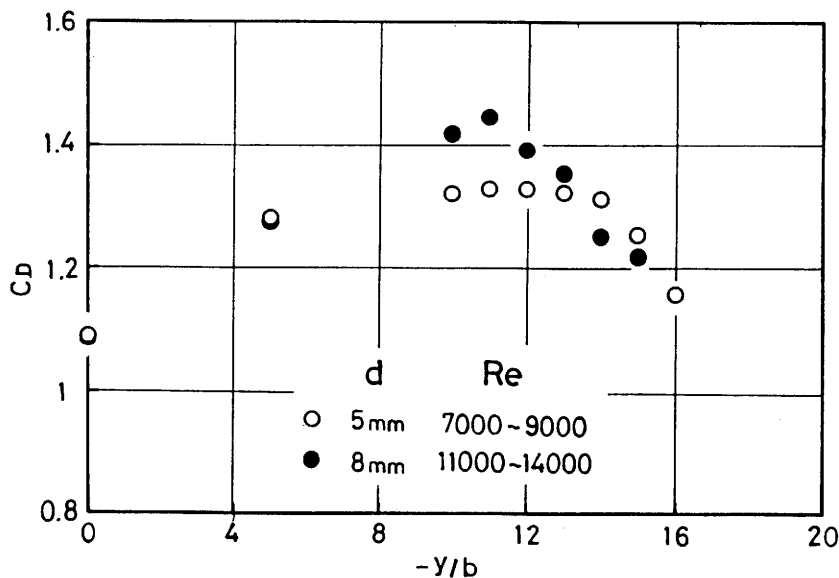


Fig. 9 Drag Coefficient Computed from Pressure Distribution

The dependance of $C_L' = C_L$ and C_D on the y direction is shown in Fig. 8 and Fig. 9, respectively. In the case that the diameter $d=5$ mm, the coefficient C_L takes negative value in the range that $-y/b = 0 \sim 0.75$, and positive values in the range that $-y/b$ is greater than 0.75. Here, the negative value of C_L means that the lift is applied on the circular cylinder in the negative y direction, that is, in the direction toward to the wall. In other words, negative C_L means that the lift is applied in the direction from the side of the higher velocity of flow to the side of the lower velocity. At the position where $-y/b = 0.75$, the value of C_L equals to zero, that is, the lift is not applied. When the circular cylinder approaches nearer to the wall ($-y/b$ becomes greater than 0.75) the lift is applied oppositely in the direction toward to the duct center. Also in the case that $d = 8$ mm, the same effects can be found. However, the difference of the experimental values of C_L between the case $d = 5$ mm and the case $d = 8$ mm is thought to be due to the effects of great blockage ratio ($d/2b$), as described in section 3.2.

As seen from Fig. 9, the dependance of C_D on the direction is so small that it may be said that C_D is independent of the velocity gradient. The value of C_D is a little greater than that for uniform flows. The reason is also thought to be due to the effects of great blockage ratio.

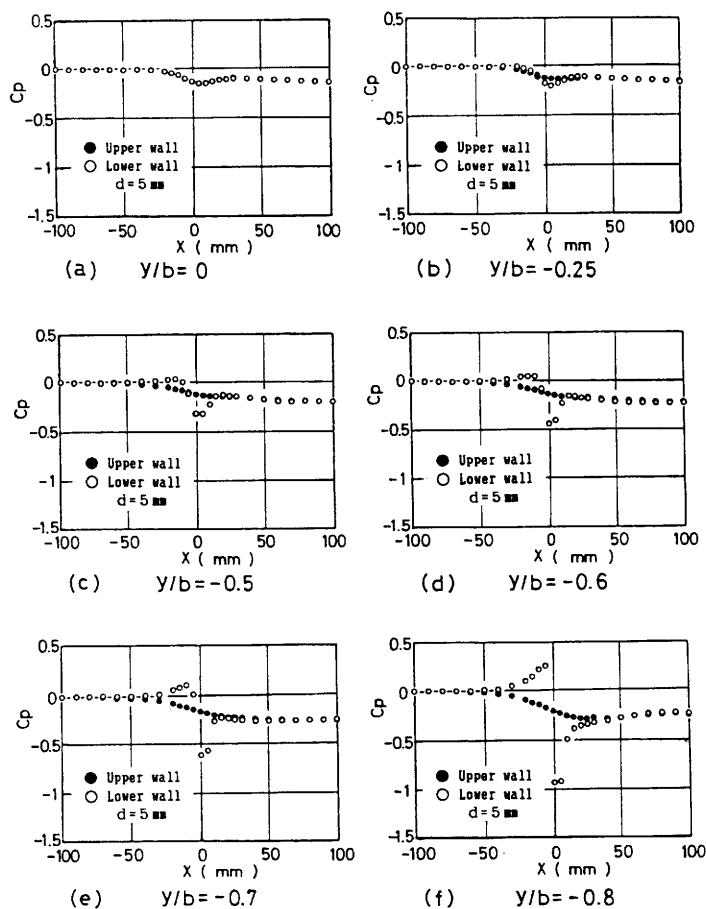


Fig.10 Pressure Distributions on Duct Walls

3.2 Pressure Distributions on the Walls of Duct

Some examples of pressure distributions on the upper and lower walls of horizontal duct are shown in Fig.10 (a) to (f). Here, the position $x = 0$ represents the center position of circular cylinder, and air flows from the negative side of x to the positive. As seen from the figure (a), when the circular cylinder is located on the duct center ($y/b = 0$), the pressure distributions on the upper and lower wall are the same, and the pressures upstream of the circular cylinder are a little higher than those downstream of it. The pressure difference between the upstream and downstream flow in the case that $d = 8$ mm (here the figure for $d = 8$ mm is omitted) is greater than in the case that $d = 5$ mm. Such pressure difference is caused by the blockage of the circular cylinder.

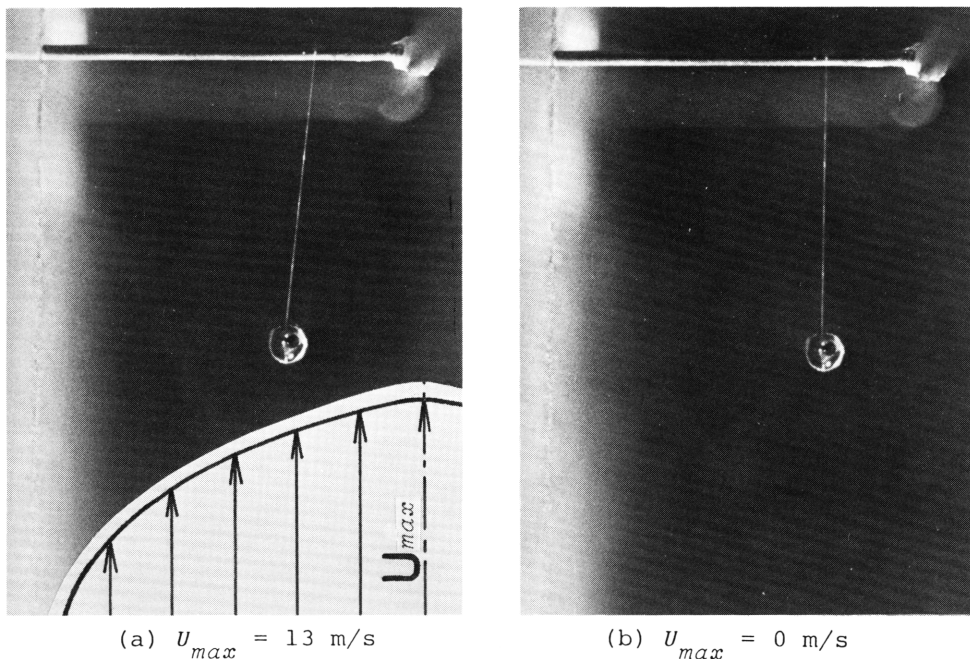


Fig.11 Photographs of a Pendant ($d = 2 \text{ mm}$)

When the circular cylinder is situated near the lower wall of duct, the pressures on the lower wall upstream of and near the circular cylinder is higher than those on the upper wall, and the pressures on the lower wall downstream of and near the circular cylinder is lower than those on the upper wall. At a section upstream of and pretty close to the circular cylinder, the pressure on the lower wall attains a maximum and at a section downstream of and close to the circular cylinder it attains a minimum. As the circular cylinder approaches closer to the wall, the pressure differences between the upper and lower wall become greater, and the region where the pressure differences are found becomes wider. Such pressure differences are related to the lift applied on the circular cylinder, but the integration of the pressure differences about the wall surface does not coincide with the lift computed from the pressure distributions on the circular cylinder.

3.3 Lift Measured by Pendant Method

Figure 11 (a) and (b) show the photographs taken in the vertical duct. Evidently, the circular cylinder is shifted from the vertical line to the duct wall. The lift coefficients obtained from the

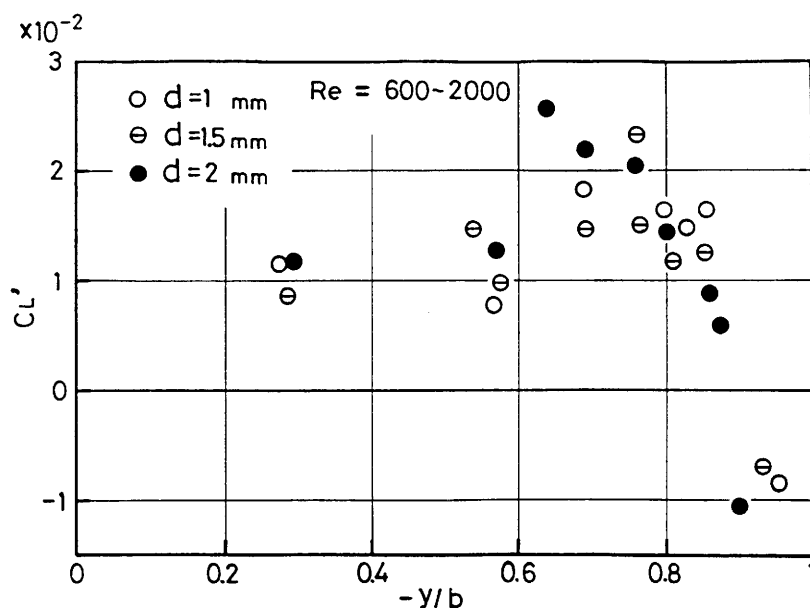


Fig.12 Lift Coefficient Obtained from Pendant Method

pendant method are shown in Fig.12. In the figure the experimental points are fairly scattered, but it may be found that the lift coefficient takes positive values in the range that $-y/b = 0 \sim$ about 0.85, and negative values in the range that $-y/b$ exceeds about 0.85. Such behavior is the same as described in section 3.1. Whereas the Reynolds number is different between the two figures, and therefore the quantitative coincidence can not be found.

4. Conclusions

The conclusions are summarized as follows:

- (1) The lift due to the flow velocity gradient is applied in the direction from the side of the higher velocity to the side of the lower velocity, and increases as the velocity gradient becomes steeper.
- (2) The lift due to the clearance between circular cylinder and duct wall is applied in the opposite direction to the lift due to the velocity gradient, and increases as the clearance becomes smaller.
- (3) The resultant lift due to the velocity gradient and due to the clearance vanishes at a clearance ratio, and turns over the applying direction across it.
- (4) The drag applied on the circular cylinder is almost independent of the velocity gradient.

References

- (1) Yamamoto, F., Bull. of JSME, 29-253 (1986), 2055.
- (2) Saito, S., J. of the Soc. of Powder Technology, Jpn, (in Japanese), 8-1 (1979), 37.
- (3) Tsuji, Y. et al., Trans. of JSME, (in Japanese), 53-474 (1986), 557.
- (4) Dennis, S. C. R., et al., J. Fluid Mech., 101-2 (1980), 257.
- (5) Laiton, J. A., ASME, AM, 48-3 (1981), 465.
- (6) Marconi, F., AIAAJ., 19-10 (1981), 1294.
- (7) Choi, Y. D. and Chung, M. K., ASME, FE, 105 (1983), 329.
- (8) Hiwada, M. et al., Trans. of JSME, (in Japanese), 52-479 (1986), 2566.